L-H transition dynamics in plasma edge turbulence simulations

L. Chôné[1,2], P. Beyer[1], Y. Sarazin[2], G. Fuhr[1], C. Bourdelle[2], S. Benkadda[1]

[1] *Aix–Marseille Université, CNRS, PIIM UMR 7345, 13397 Marseille Cedex 20, France*

[2] *CEA, IRFM, F-13108 Saint-Paul-lez-Durance, France*

Achieving a large energy confinement is critical to the viability of magnetic fusion. This represents a great challenge as the plasma of magnetic machines is largely unstable, notably due to the presence of large gradients, resulting in widespread turbulence and fast energy losses. Experiments however show that under certain circumstances, the plasma self-organises into a state characterised by large, localised $\mathbf{E}\times\mathbf{B}$ shear flows that quench turbulence, creating a transport barrier. Such transport barriers provide an important gain in confinement, therefore H-mode, characterised by an external transport barrier (ETB) near the edge of the plasma, is used by the reference scenario for ITER and ulterior machines. Theoretical understanding of the transition to H-mode remains however unresolved [1], putting large uncertainties on the value of the L-H transition power threshold [2]. H-mode is furthermore often accompanied by relaxation oscillations of the ETB called edge-localised modes (ELMs), which put significant stresses on the plasma facing components if not mitigated, making full understanding of the phenomenon all the more desirable.

In this work, we use flux-driven 3D simulations of edge turbulence to search for the mechanism responsible for generating the mean flow causing the ETB. The extended reduced MHD model used in the EMEDGE3D code to describe resistive ballooning (RBM) turbulence is the following [3]:

$$\partial_t \nabla_\perp^2 \phi + \{\phi, \nabla_\perp^2 \phi\} = -\nabla_\parallel^2 \phi - \mathrm{G}p + \partial_x F_{neo} + \nu_\perp \nabla_\perp^4 \phi \quad (1)$$

$$\partial_t p + \{\phi, p\} = \delta_c \mathrm{G}\phi + \chi_\parallel \nabla_\parallel^2 p + \chi_\perp \nabla_\perp^2 p + S(x) \quad (2)$$

This model is electrostatic and simulates turbulence in the edge, up to the last closed flux-surface (LCFS). The scrape-off layer physics is not included. Equations (1,2) are respectively the charge balance and energy balance, with the two fields ϕ and p being the electric potential and the total pressure. $\nabla_\parallel$ and $\nabla_\perp$ are respectively the parallel and perpendicular gradients with respect to the magnetic field lines. It follows that $\nabla_\perp^2\phi$ is the vorticity of the $\mathbf{E}\times\mathbf{B}$ flow. G is a toroidal curvature operator, and Poisson brackets $\{\phi,\cdot\}$ account for the advection by the electric drift velocity. In Eq.1, $\nu_\perp$ accounts for the classical viscosity, while in Eq.2, $\chi_\perp$ and $\chi_\parallel$ are respectively the perpendicular and parallel collisional heat diffusivities. The F_neo accounts for collisional relaxation of the flow towards the neoclassical value due to friction between

trapped and passing particles, and will be detailed below.

The system (1,2) is normalised as follows: time is normalised to the interchange time $\tau_{int} = \frac{\sqrt{R_0 L_p}}{\sqrt{2} c_{S0}}$ with $c_{S0} = \sqrt{\frac{p_0}{n_0 m_i}}$ the typical acoustic speed and L_p the typical pressure gradient length. The perpendicular length scale is the resistive ballooning length $\xi_{bal} = \sqrt{\frac{\rho \eta_\parallel}{\tau_{int}}} \frac{L_s}{B_0}$, with the magnetic shear length L_s being the parallel length scale. The fields ϕ and p are normalised respectively to $\frac{B_0 \xi_{bal}^2}{\tau_{int}}$ and $\frac{\xi_{bal} p_0}{L_p}$.

One can start the reasoning leading to the friction term F_{neo} from the radial force balance equation for ions. Here, in the framework of our model, we have to make several assumptions: first, we consider the density as constant $n = n_0$, and second we assume a constant ratio between the ion and electron temperatures $T_i = \varepsilon_T T_e$. Furthermore, we consider that toroidal rotation is small (generally true in the absence of torque injection). The radial force balance is then written thus:

$$\partial_x \bar{\phi} + \frac{\varepsilon_T}{\varepsilon_T + 1} \frac{\tau_{int} p_0}{\xi_{bal} L_p e n_0 B_0} \partial_x \bar{p} \quad = \quad \bar{u}_y \tag{3}$$

Where $\bar{\phi} = \phi - \tilde{\phi}$ and $\bar{p} = p - \tilde{p}$ indicate flux-surface averaged quantities, with $\tilde{\phi}$ and $\tilde{p}$ the associated perturbations.

The neoclassical poloidal velocity is given by: $\bar{u}_y^{neo} = \frac{\varepsilon_T}{\varepsilon_T + 1} \frac{\tau_{int} p_0}{\xi_{bal} L_p e n_0 B_0} K(\nu_{i,*}) \partial_x \bar{p}$ [4, 5], with $K(\nu_{i,*})$ comprised between -2.1 in the Pfirsch-Schlüter regime and 1.17 in the banana regime (in the limit of large aspect ratio), and varying sharply with collisionality between the two.

Eq.3 couples the pressure gradient and the $\mathbf{E} \times \mathbf{B}$ velocity $\partial_x \bar{\phi}$. This coupling is then introduced in Eq.1 through a heuristic closure, taking the form of a friction term [6, 7]:

$$F_{neo} = -\mu_{neo}(\bar{p}) \left[\partial_x \bar{\phi} - K_{neo}(\bar{p}) \partial_x \bar{p} \right] \tag{4}$$

Through the coupling of the $\mathbf{E} \times \mathbf{B}$ velocity and the pressure gradient in F_{neo}, a feedback loop can occur that would lead to strong flows and turbulence stabilisation: local stabilisation of turbulence would cause a steepening of the pressure gradient, resulting in a strengthening of the $\mathbf{E} \times \mathbf{B}$ shear flow, stabilising turbulence and further steepening the pressure gradient, with again an effect on the flow. The coefficients μ_{neo} and K_{neo} influence greatly the shape of the $\mathbf{E} \times \mathbf{B}$ velocity profile and control whether the feedback loop can produce a self-generated transport barrier or not. Both coefficients μ_{neo} and K_{neo} depend on the collisionality, i.e. in our model on the flux-surface averaged pressure $\bar{p}$, at each radial position and each time-step. Taking into account those spatial and temporal variations is found to be a key element in our simulations, allowing for the spontaneous formation of a transport barrier above a certain threshold of input power (illustrated in Figure 1 and further discussed in [7]). Similar simulations using constant

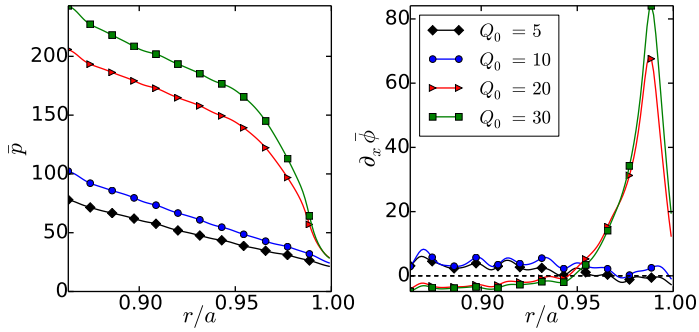

Figure 1: Pressure (left) and $\mathbf{E} \times \mathbf{B}$ velocity (right) radial profiles for different values of input power. These profiles show the generation of a transport barrier above a threshold in Q_0. The profiles are averaged over several hundred interchange times.

μ_{neo} and K_{neo} have not showed the generation of a transport barrier, despite a noticeable impact of the friction term on the flow dynamics. As can be seen in Fig.1, when crossing the threshold of input power, the $\mathbf{E} \times \mathbf{B}$ velocity profile changes from low-amplitude with some corrugations to a sharply peaked profile near the last closed flux-surface. This peak is surrounded by regions of stabilising shear causing a transport barrier, with a noticeable effect on the pressure profile.

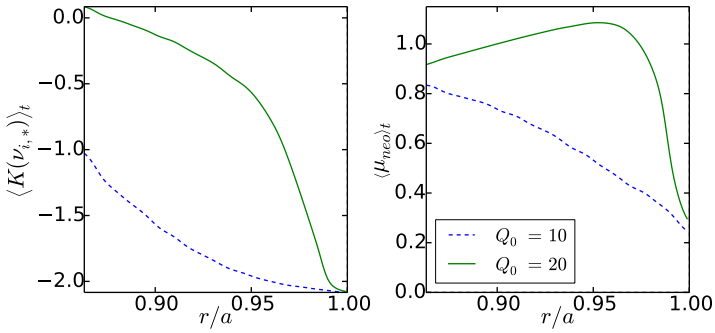

Figure 2: Radial profiles of the coefficients K_{neo} (left) and μ_{neo} (right) before and after the formation of the barrier. The profiles are averaged over several hundred interchange times.

Looking at the profiles of μ_{neo} and K_{neo} below and above the transition threshold (Fig.2), one can see that the two change drastically: the K_{neo} profile steepens at the position of the barrier (much like the pressure profile), and a maximum appears on the profile of μ_{neo} at the position of the barrier. The radial variations of K_{neo} are responsible for the generation of a strong $\mathbf{E} \times \mathbf{B}$ velocity shear, while the flow is effectively forced to the neoclassical value at the position of the μ_{neo} peak [7].

It is interesting to note that the barrier is not always quiescent, but can exhibit a complex dynamics. In particular, close to the transition threshold, the barrier relaxes quasi-periodically. This was already suggested using a simplified 1D model [8, 7], and is now confirmed by the 3D

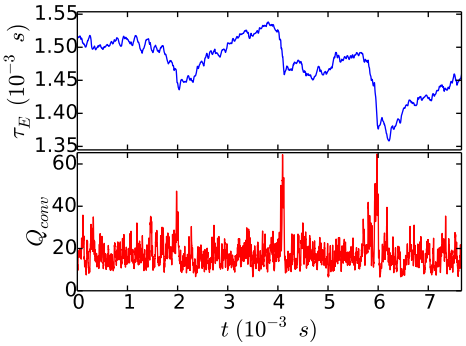

Figure 3: Relaxations of the barrier, for $Q_0 = 19$. The top panel shows the time evolution of the energy confinement time $\tau_E = 1/Q_0 \int_x \bar{p} \mathrm{d}x$, the bottom row shows the convective flux at the position of the barrier.

simulations. The relaxation oscillations of the barrier exhibit similarities with type-III ELMs: they appear close above the power threshold, with a frequency decreasing with power up to the point of vanishing completely. They are governed by resistive modes, as are type-III ELMs [9]. Such relaxations have already been observed in 3D simulations with imposed shear flows, and a mechanism was proposed [10].

In conclusion, we report results of 3D simulations of edge turbulence showing self-generation of a transport barrier above a threshold of input power. The barrier obtained thus exhibits several features of the H-mode ETB, notably relaxations oscillations with similarities to type-III ELMs.

This work is supported by the French National Research Agency, project ANR-2010-BLAN-940-01. This work was granted access to the HPC resources of Aix-Marseille Université financed by the project Equip@Meso (ANR-10-EQPX-29-01) of the program «Investissements d'Avenir» supervised by the Agence Nationale pour la Recherche. This work, supported by the European Communities under the contract of Association between Euratom and CEA, was carried out within the framework of the European Fusion Development Agreement. The views and opinions expressed herein do not necessarily reflect those of the European Commission.

References

[1] J. W. Connor *et al.*, Plasma Phys. Control. Fusion **42** (2000) R1–R74.

[2] Y. R. Martin *et al.*, J. Phys.: Conf. Ser. **123** (2008) 012033.

[3] G. Fuhr *et al.*, Phys. Rev. Lett. **101**, 195001 (2008).

[4] F. L. Hinton *et al.*, Rev. Mod. Phys. **48**, 239 (1976).

[5] P. Helander *et al.*, Collisional Transport in Magnetized Plasmas, Cambridge University Press (2005).

[6] T. A. Gianakon *et al.*, Phys. Plasmas **9**, 536 (2002).

[7] L. Chôné *et al.*, to be published in Phys. Plasmas.

[8] S. Benkadda *et al.*, Nucl. Fusion **41** (2001) 995.

[9] W. Suttrop, Plasma Phys. Control. Fusion **42** (2000) A1–A14.

[10] P. Beyer *et al.*, Phys. Rev. Lett. **94**, 105001 (2005).